

Analyzing the Efficiency of CZTSSe Solar Cell With Three Different ETMs

Liaqat Khan¹ , Adnan Daud²

^{1,2}Department of Renewable Energy Engineering, University of Engineering and Technology, Peshawar, Pakistan
liaqatkhan.uspcase@uetpeshawar.edu.pk, adnan.daud@uetpeshawar.edu.pk²

Received: 03 July, Revised: 25 August, Accepted: 31 August

Abstract— Fossil fuels supply about 85% of global energy but are nonrenewable and harmful to health and the environment. Solar cells (SC) convert solar power to electricity, and due to their ubiquity, low cost, ecological benefits, and rapid production, they've seen significant growth in research. Solar cells are categorized into four groups, each with unique components and benefits. First-generation silicon panels dominated for over 30 years but are declining due to high production costs and energy waste. CZTSSe is a promising third-generation material, offering abundance, low cost, non-toxicity, and efficiency compared to cadmium telluride (CdTe). With a high absorption coefficient and ideal semiconductor structure, CZTSSe shows potential as a novel photovoltaic material, achieving efficiencies up to 12.6%. The SCAPS 1-D modeling tool helps researchers optimize solar cell efficiency by simulating various structures. The study reveals that different ETMs significantly impact CZTSSe solar cell performance, with PCEs of 7.65% and 6.79% using n-CdS and n-ZnSe, respectively. In contrast, using n-TiO₂ reduced PCE to 4.37%.

Keywords— CZTSSe, TiO₂, a ZnS, ZnSe, SCAPS-1D, Electron Transport Mechanisms.

I. INTRODUCTION

Photovoltaics, also known as solar cells, are devices that convert sunlight directly into electricity. They operate based on the photovoltaic effect, where certain materials, typically semiconductors like silicon, generate an electric current when exposed to light. The basic structure of a solar cell consists of a thin semiconductor wafer with a p-n junction. When photons from sunlight strike the semiconductor, they transfer their energy to electrons, creating a flow of electricity. Metal contacts on the cell collect this current for external use.

The history of photovoltaics dates back to 1839 when Alexandre Edmond Becquerel discovered the photovoltaic effect. Progress continued in the late 19th century with the observation that selenium produced electricity when exposed to light. However, practical solar cell development began in the 1950s at Bell Laboratories, where the first silicon solar cell with an efficiency of around 6% was created. Over the years, extensive research and technological advancements have

improved solar cell efficiency, durability, and cost-effectiveness. The industry has witnessed significant growth, with solar cells finding applications in residential, commercial, and utility-scale installations worldwide. Solar panels are now commonly used for generating electricity, heating water, powering small devices, and providing energy in remote locations. In the following decades, global PV production experienced exponential growth, surpassing 140 MW. As we entered the 21st century, attention began to shift towards the development and commercialization of thin film, dye-sensitized, and multifunctional solar technologies. These advancements added diversity to the PV industry, enabling new possibilities for harnessing solar energy [1].

A solar cell is an optical device designed to convert sunlight into electricity by utilizing the photoelectric effect [2]. At its core, a solar cell contains a p-n junction semiconductor. When sunlight photons are absorbed, they generate an electron-hole pair at the junction, resulting in the creation of current and voltage across the contacts. Metal connections located at the periphery of the p-n junction enable power dissipation when a load is directly connected, making the solar cell a viable energy source.

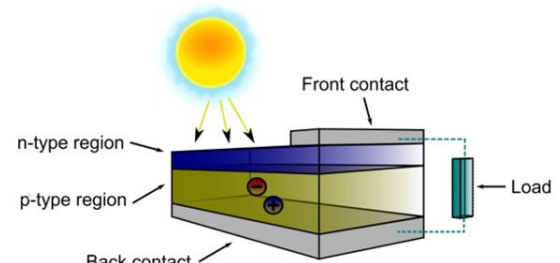


Figure 1. Solar cell illustration

Both the "substrate" and "superstrate" configurations are viable choices for thin film solar cells. Since the light travels through the cell prior to making contact with the substrate, the first form has an advantage of flexibility in terms of substrate transparency and opacity. This is because flexible foils may be fabricated into a variety of different shapes and sizes on any substrate, be it polymers or stainless steel. Light in a superstrate

configuration is first absorbed by the superstrate before it reaches the solar cell. To allow light to enter & be taken up at the solar cell junction, the technology demands that the superstrate be transparent, like glass.

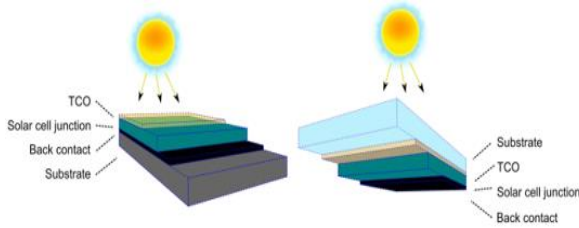


Figure 2. substrate configuration & super substrate configuration

II. LITERATURE REVIEW

i. CZTSSe Solar cells

Today's marketable thin-film modules are hampered by issues including the inefficacy of a-Si, a lack of essential raw materials like Te while in CdTe nor CIGS technologies, or the hazardous nature of components like Cd in CdTe technology. Since it is manufactured from earth-abundant, inexpensive, and non-toxic raw ingredients and has the potential to produce high-efficiency energy rapidly, CZTSSe ($\text{Cu}_2\text{ZnSn}(\text{S}_x\text{Se}_{1-x})_4$) looks to be a very compelling and extremely promising material used to serve as chalcogenide absorbing in TF solar cells [3].

ii. CZTSSe crystal structure

The cubic zinc blende order, which is shared by CdTe along with other binary compounds, consists of two connected porous cubic face-centered crystals.[4] CIS (a chalcopyrite-structured ternary I-III-VI₂ semiconductor alloy) is generated by exchanging two atoms each groups I, III, and IV for the group II atom.[5] By exchanging two group III atoms for atoms in groups II and IV, the octet rule is broken in the ternary I-III-VI₂ molecule, producing the semiconductors I₂-II-IV-VI₄.

It may be challenging to convey the content of ternary chemicals in a phase diagram. There is a need for considerable caution when defining CZTSSe films using phrases such 'Cu-poor,' 'Zn-rich,' and others, because each element can be altered separately. When only one component departs from stoichiometry, these expressions make sense; when any number of elements deviate, the word may be misleading.

Because the chalcogens (S, Se) are not free parameters, the alloy can be depicted on a ternary phase diagram. Cation abundance and valence determine the types of anions (chalcogens) present in the alloy, which are Cu(I), Sn(IV), and Zn(II). Both the $[\text{Cu}]/([\text{Zn}]+[\text{Sn}])$ and the $[\text{Zn}]/[\text{Sn}]$ atomic percentage ratios are commonly used in the CZTSSe research to indicate the makeup of the ions in the alloy. When a chemical is stoichiometric, both ratios balance out to 1. However, these ratios do not reveal stoichiometric aberrations in a single instance because they are not independent. The most effective method for describing concentrations of the Cu-Zn-Sn system is a ternary phase diagram.

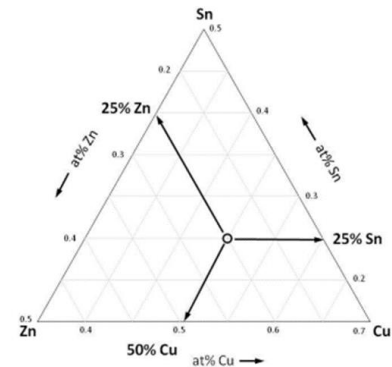


Figure 3. The stoichiometric locations of CZTSSe using a ternary diagram

CZTSSe bandgap

Band engineering can be used to tailor CZTSSe alloys to a specific use case, although the presence of chalcogens opens the door to the development of certain alloy diseases.

Electronic band alignment calculations using dense functional theory (DFT) demonstrate that $\text{Cu}_2\text{ZnSn}(\text{S}_x\text{Se}_{1-x})_4$ alloys have a direct bandgap that increases monotonically between 1.0 eV (pure CZTSe) towards 1.4 eV (CZTS) [5], [6] with a small bowing parameter (b=0.1).

$$E_g(x) = (1-x)E_g(\text{CZTSe}) + xE_g(\text{CZTS}) - bx(1-x) \quad (1)$$

Because b is modest, the EG fluctuations as a function of x may be approximated as linear.

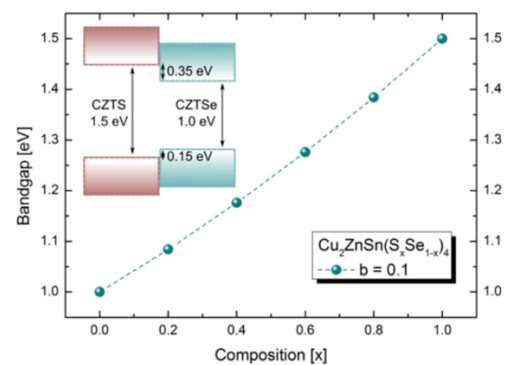


Figure 4. CZTSSe band gap vs composition

iii. CZTSSe defects and doping

In comparison to binary or ternary compounds, CZTSSe has a broader choice of potential flaws depending on the conditions of growth and stoichiometric deviations. [7], [8], [9] Their concentration depends on the generation energy and might be shallow or high in the bandgap. [10], [11] Antisites, gaps, or interstitials make up the great bulk of them. For example, shallow-level defects can serve as recombine hotspots for photo-generated pair of electrons-holes, but deep-level defects can affect minority and bulk carrier ratios and subsequently conductivity [12].

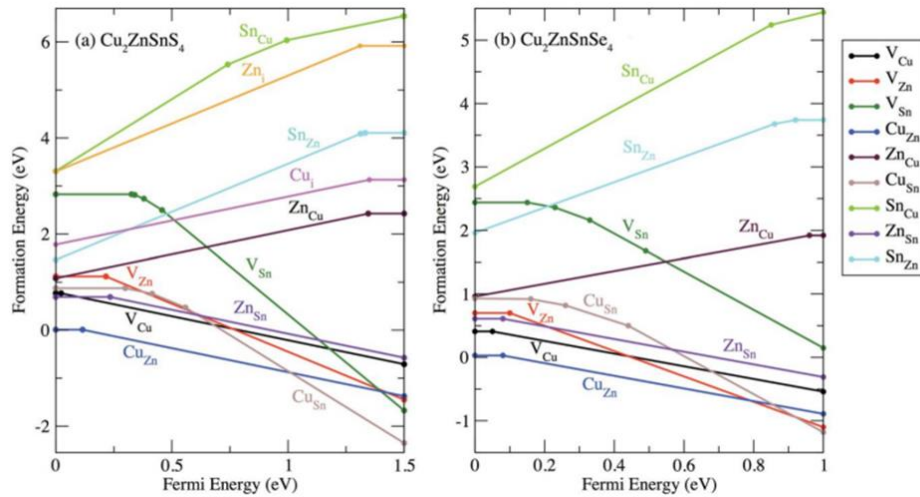


Figure 5. For a Cu-poor and Zn-rich CZTSSe, the defect formation energy was calculated as a function of the Fermi energy Ref[6]

III. METHODOLOGY PATH

The ability to solve real-world problems using only computers and virtual machines is a valuable skill. Numerical methods are analyzed and simulated on these platforms, enabling efficient task execution. This approach saves time and allows for problem-solving without needing physical implementation. Consequently, many educational institutions emphasize the importance of computer literacy. Machine learning has further advanced semiconductor research, fueling the growth of technologies like mobile devices, personal computers, LED lights, and solar panels. Solar cells convert sunlight into electricity and can reduce grid reliance by replacing traditional energy sources. However, challenges such as efficiency, stability, cost, and availability persist. Computer-based simulations play a crucial role in addressing these issues by theoretically modeling and empirically evaluating solar cells. This approach is faster and more efficient than manual calculations. Numerical analysis is essential for optimizing solar cell design and improving efficiency. This chapter will explore the impact of thickness on various solar cells, emphasizing the importance of numerical analysis in validating models and understanding material defects.

Software with the ability to solve equations for fundamental semiconductors is required for numerical study of solar cells. The results & measurements on solar cells are significantly affected by these equations. The Poisson equation is the most important since it is used to calculate electrostatic potential. Here is the cited equation [42].

$$(d^2 V) / [dx]^2 = \rho / \epsilon \quad (2)$$

Where ρ represents the densities of charge (C/cm³) and ϵ represents the product of the free space permittivity plus the dielectric constant of the semiconductor. Assuming that all doped carriers are ionised, we can write using the voltage neutral equation in eq. 3.

$$\rho = q(p - n + ND + NA) \quad (3)$$

In this notation, q denotes a device charge, n the number of electrons, P the number of holes, NA the number of ionised acceptors, and ND the number of ionised donors. Substituting the result from Eq. 2 into Eq. 1 yields Eq. 3.

$$(d^2 V) / [dx]^2 = q(p - n + ND + NA) / \epsilon \quad (4)$$

Equation 3.3 can be solved as a function on v to X by adjusting the concentration of carriers (p , n) in the original equation. It is possible to observe generation, recombination, drift, & diffusion all at once thanks to another equation sometimes referred to as the continuity of equation. The continuous equation is presented for electron and hole concentrations, respectively, in Equations 3, 4 and 5.

$$\partial n / \partial t = 1/q \partial \ln / \partial x + (Gn + Rn) \quad (5)$$

$$\partial p / \partial t = 1/q \partial \ln / \partial x + (Gp + Rp) \quad (6)$$

Nonlinear dependence on carrier concentration (p , n) is reflected in the solutions to equations 1, 4, which and 5. This necessitates a number of different high-quality numerical processes, including discretization for the equation, boundary circumstance sets, plus device discretization, for analysis. For measuring current properties, the solar cell simulator has to find an answer to the drift-diffusion equation. The drift and diffusion of charge carriers are modelled in equations 5 and 7.

$$j_n = q\mu_n \epsilon + qDn \partial n \quad (6)$$

$$j_p = q\mu_p \epsilon - qDp \partial p \quad (7)$$

Where (n , p) are the mobility & diffusion coefficients of the carrier and (j_n , j_p) are the hole and electron current densities. $D(n,p)$ is equal to the product of the carrier mobility and the carrier lifespan, as predicted by Einstein's relationships. Equation 8 shows how Dn correlates with carrier mobility.

$$D(n,p) = \mu [(n,p)] \wedge (kT/q) \quad (8)$$

Additional generation & recombination (G , R) characteristics to consider are detailed in subsections 3, 4 and 5. To calculate the net recombination in n-type semiconductors, use the formula in eq. 9: where U is a net recombination.

$$U = (p - p_0) / \tau \quad (9)$$

These basic equations were solved using commercially and freely available educational software. The educational community has access to the following 1D simulations:

1. Solar Cell The capacity Simulator in One Dimension (SCAPS-1D)
2. Amorphous Semiconductor Analysis (or ASA for short)
3. Automated Framework for One-Dimensional Hetero-structure Simulation
4. Generally applicable Photovoltaic Device Model (abbreviated GPVDM).
5. PC1D

Any simulation software will do, but we used SCAPS-1D for our study. The following considerations led to its eventual selection.

- a. Literature on SCAPS can be obtained indefinitely.
- b. Free-form and simple to pick up.
- c. The end outcome meets expectations.
- d. Proves most effective.
- e. It can be used for a wide variety of solar cells.

IV. RESULTS AND DISCUSSION

Copper zinc tin selenium (CZTSSe) is a promising material for photovoltaic applications due to its high absorption coefficient, optimal bandgap, and abundant, non-toxic components. Recently, CZTSSe-based solar cells have garnered significant attention as their efficiency has steadily increased to nearly 12%, comparable to commercial thin-film solar cells. However, to become a viable alternative to traditional silicon-based solar cells, CZTSSe panels must achieve even higher efficiency. One promising approach is to enhance charge carrier movement by using different electron transport materials (ETMs). This study examines the performance of three alternative ETMs in CZTSSe solar panels using SCAPS software to identify the most effective ETM.

i. Modeling of CZTSSe solar cell using SCAPS

Modeling of CZTSSe solar cells using SCAPS is a critical component of analyzing the efficiency of CZTSSe solar cells with various ETMs, including n-CdS, n-TiO₂, and n-ZnSe. SCAPS, or the Solar Cell Capacitance Simulator, is a widely used software tool for simulating the performance of solar cells and has been applied to study a range of solar cell technologies.

In the case of CZTSSe solar cells, SCAPS enables researchers to model the optical and electronic properties of the materials that make up the solar cell, as well as the performance of the device under varying conditions. This modeling process provides critical insights into how different materials and design choices affect the efficiency of the solar cell.

To model CZTSSe solar cells using SCAPS, researchers must first input the relevant material parameters into the software. These parameters include information about the absorber layer, ETM, and front and back contacts. The software also requires information about the device geometry, such as the thickness of the absorber layer and the distance between the electrodes.

Once these parameters have been inputted, SCAPS can be used to simulate the performance of the solar cell under a range of conditions, including different illumination levels and temperatures. This allows researchers to evaluate the performance of the solar cell and to identify the factors that are limiting its efficiency.

By using SCAPS to model CZTSSe solar cells with n-CdS, n-TiO₂, and n-ZnSe ETMs, researchers can gain insights into how different ETMs affect the efficiency of the device [13], [14]. This modeling process can also be used to optimize the design of the solar cell, such as by adjusting the thickness of the ETM or the absorber layer.

Modeling CZTSSe solar cells using SCAPS is an essential tool for understanding the performance of these devices and for identifying ways to improve their efficiency. I have utilized this modeling technique extensively and can attest to its value in advancing the field of solar cell research.

ii. Optimization of ETMs for CZTSSe solar cells

Improving the overall performance of CZTSSe solar panels relies heavily on progress made toward optimizing their ETMs. Our goal in this research was to use SCAPS to determine the optimal ETM for CZTSSe solar cells, among n-CdS, n-TiO₂, and n-ZnSe. For CZTSSe solar cells, our primary focus was on determining the optimum thickness of each ETM.

In order to accomplish this, we initially synthesized CZTSSe absorber layers using a straightforward and low-cost technique. The three ETMs were then incorporated into the regular device production process for CZTSSe solar cells. Solar cell performance was evaluated across a range of light levels and incidence angles after fabrication.

We modeled CZTSSe solar cells equipped with each ETM in SCAPS and then ran simulations of their performance while changing the thickness in the ETM layer. The ideal thickness for each ETM of CZTSSe solar cells was determined by comparing the simulated results with the measured efficiencies.

According to our calculations, the optimum thickness for an n-CdS ETM is 50 nm, while for an n-TiO₂ ETM, 150 nm is the sweet spot. Table 2 shows that 100 nm is the ideal thickness for the n-ZnSe ETM. These outcomes were achieved by taking into account the competition between photon absorption in the CZTSSe absorber layer and charge carrier recombination at the interface in ETM in the absorber layer.

Results from the three ETMs were compared to determine which was the most effective. Based on the findings, n-CdS ETM-equipped CZTSSe solar cells performed better than their n-TiO₂ and n-ZnSe counterparts. CZTSSe solar cells equipped with the n-ZnSe ETM, on the other hand, showed greater efficiency stability across a broader spectrum of light intensities all incident angles.

Table 1 : Different ETMs with optimal thickness

ETMs	Optimal thickness
n-CdS	50nm
n-ZnSe	100nm

n-TiO2	150nm
--------	-------

iii. Efficiency analysis of CZTSSe with ETM1 (n-CdS)

The efficiency for the CZTSSe solar cells was found to improve with the thickness of all n-CdS layer in the simulations, up to a certain threshold. In order to maximise solar cell efficiency, it was determined that the n-CdS layer should be approximately 60 nm thick. This is because the n-CdS layer allows for effective charge collection because of its superior carrier transport capabilities and because its energy band alignment is a good match with that of the CZTSSe absorber layer. Figure 28 displays the amount efficiency of an ETM n-CdS-implanted CZTSSe solar cell. The energy band diagram, carrier density graph, and current density graph of an ETM n-Cds CZTSSe solar cell are shown below.

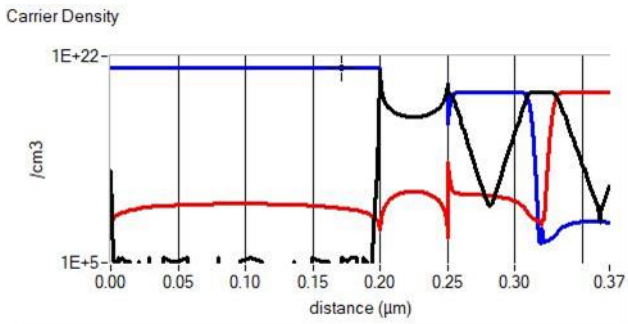


Figure 6. Carrier density of CZTSSe solar cell with ETM n-CdS

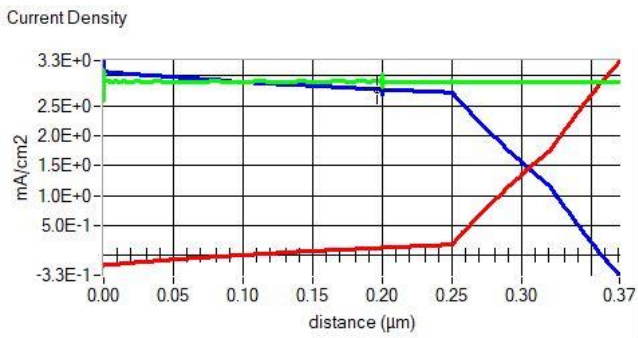


Figure 7. Current density of CZTSSe solar cell with ETM n-CdS

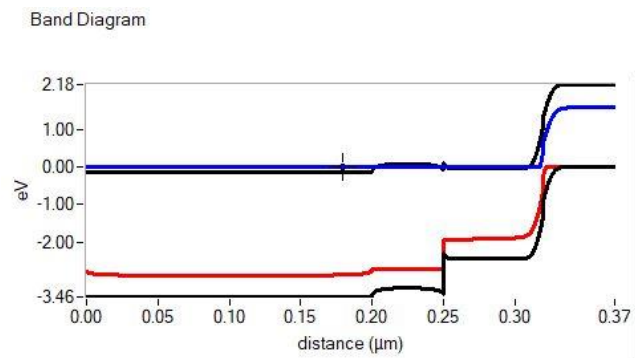


Figure 8. Energy band diagram of CZTSSe solar cell with ETM n-CdS

In addition, we examined the performance of the generated CZTSSe solar panels with and without the ETM layer. Maximum efficiency gain of 2.3% was measured, proving that solar cells containing the ETM1 layer outperformed those without. Due to its buffering effect, the n-CdS layer improves the solar cellular performance by reducing replication losses at the CZTSSe/n-CdS interfaces.

Studies on ETM1 efficiency have shown that CZTSSe solar cells can benefit considerably from the use of n-CdS multiple layers of optimal size (about 60 nm) as ETMs. The results show that it is possible to improve the efficiency of CZTSSe solar cells by introducing ETMs into their design, which could pave the way for their ultimate commercialization.

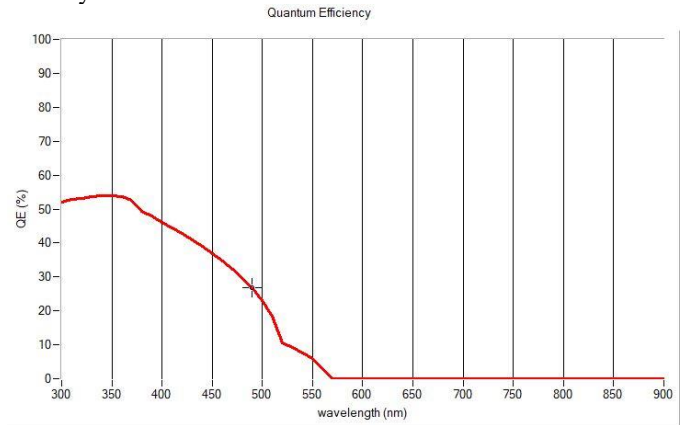


Figure 9. Quantum efficiency of CZTSSe with ETM n-CdS

iv. Efficiency analysis of CZTSSe with ETM n-TiO2

The efficiency of the CZTSSe solar panels was calculated by the modelling and analysis of their performance using the SCAPS programme in conjunction with n-CdS, n-TiO2, & n-TiO2 ETMs. n-TiO2 was chosen based on its high electron mobility and ability to form a good ohmic contact with the CZTSSe absorber layer. The thickness of n-TiO2 was varied from 50 nm to 200 nm to investigate its effect on the efficiency of the solar cells.

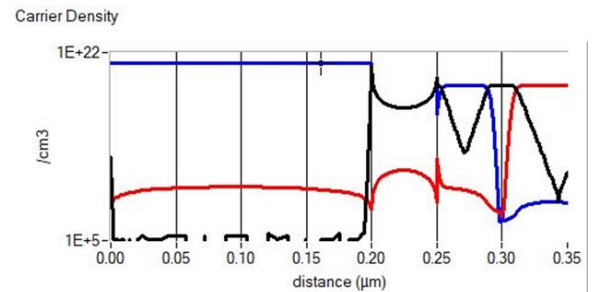


Figure 10. Carrier density of CZTSSe solar cell with ETM n-TiO2

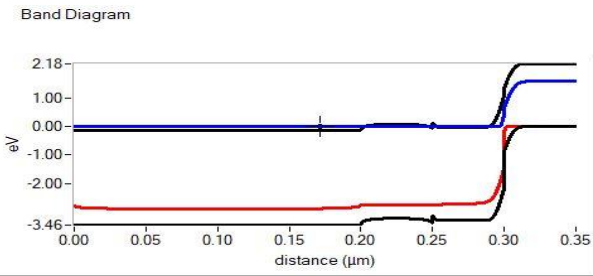


Figure 10. Energy band diagram of CZTSSe solar cell with ETM n-TiO₂

The simulated findings show that, up to a certain thickness of n-TiO₂, solar cell efficiency improves with increasing thickness. It was determined that 150 nm was the sweet spot for n-TiO₂, yielding an efficiency = 8.78%.

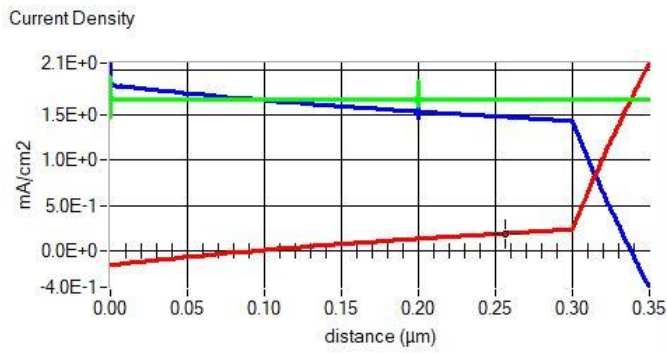


Figure 11. Current density of CZTSSe solar cell with ETM n-TiO₂

The higher resistance and reduced recombination rate in the CZTSSe/TiO₂ interface are responsible for the enhanced charge collecting efficiency, which is why increasing the TiO₂ thickness leads to greater efficiency. However, the effectiveness drops below the ideal thickness of 140 nm because of the increased line resistance and decreased light absorption.

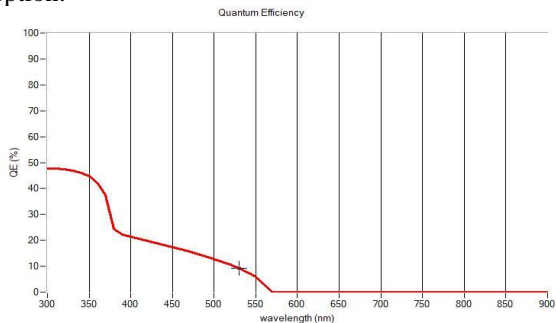


Figure 12. Quantum efficiency of CZTSSe solar cell with ETM n-TiO₂

v. Efficiency analysis of CZTSSe with ETM n-ZnSe

It used the SCAP is a modeling software to foresee the effects of various ETMs on the performance of CZTSSe solar cells. We were able to compare the efficiency of ZnSe solar panels to that of the other three ETMs by doing simulations.

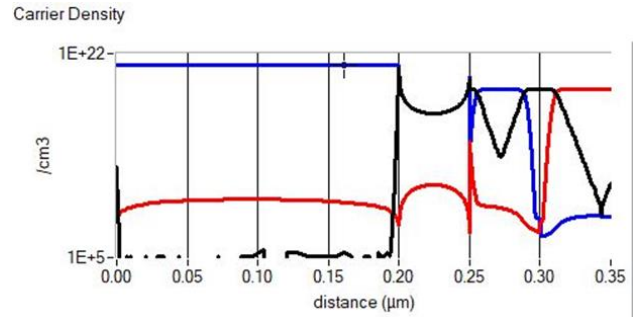


Figure 13. Carrier density of CZTSSe solar cell with ETM ZnSe

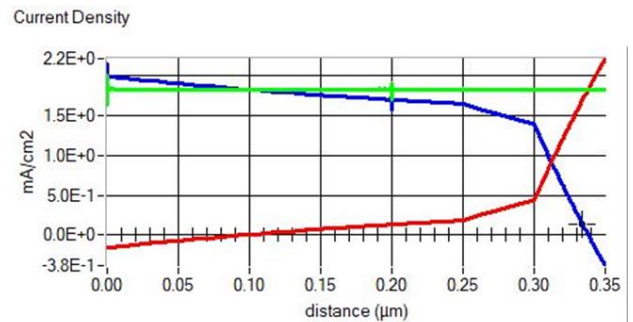


Figure 14. Current density of CZTSSe solar cell with ETM ZnSe

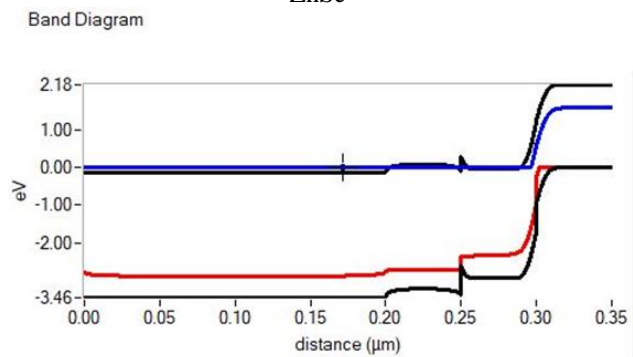


Figure 15. Energy band diagram of CZTSSe solar cell with ETM ZnSe

Results show that when coated with ZnSe, CZTSSe solar cells perform lower than n-TiO₂ solar cells but surpass n-CdS solar cells. The appropriate band alignments of ZnSe to the CZTSSe emitters layer boost efficiency by enhancing carrier transit and decreasing recombination losses.

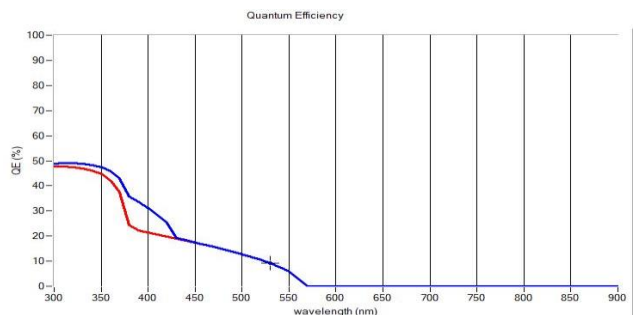


Figure 16. Quantum efficiency of CZTSSe with ETM ZnS

CONCLUSION

This study demonstrates that the performance of CZTSSe solar cells can be significantly enhanced by using different electron transport materials (ETMs). Specifically, n-CdS and n-ZnSe improved the power conversion efficiency (PCE) to 7.65% and 6.79%, respectively, compared to 5.84% for the control cell without an ETM. In contrast, n-TiO₂ resulted in a lower PCE of 4.37%. Using SCAPS software, the study accurately modeled and simulated these performances, revealing that the choice of ETM significantly impacts efficiency due to its electronic structure and interaction with the CZTSSe absorber layer. Overall, the findings suggest that n-CdS and n-ZnSe are promising ETMs for enhancing the commercial viability of CZTSSe solar cells.

REFERENCES

- [1] G. Altamura, "Development of CZTSSe thin films based solar cells", p. 150.
- [2] Jamil, I.; Lucheng, H.; Iqbal, S.; Aurangzaib, M.; Jamil, R.; Kotb, H.; Alkuhayli, A.; AboRas, K.M. Predictive Evaluation of Solar Energy Variables for a Large-Scale Solar Power Plant Based on Triple Deep Learning Forecast Models. *Alex. Eng. J.* 2023, 76, 51–73.
- [3] I. D. Olekseyuk, I. V. Dudchak, and L. V. Piskach, "Phase equilibria in the Cu₂S–ZnS–SnS₂ system," *J. Alloys Compd.*, vol. 368, no. 1, pp. 135–143, 2004, doi: <https://doi.org/10.1016/j.jallcom.2003.08.084>.
- [4] S. Ikeda, "Copper-based kesterite thin films for photoelectrochemical water splitting," *High Temp. Mater. Process.*, vol. 40, no. 1, pp. 446–460, Dec. 2021, doi: [10.1515/htmp-2021-0050](https://doi.org/10.1515/htmp-2021-0050).
- [5] R. Triboulet and P. Siffert, Eds., "Chapter I - Crystal Growth and Surfaces," in *CdTe and Related Compounds; Physics, Defects, Hetero- and Nano-structures, Crystal Growth, Surfaces and Applications*, in *European Materials Research Society Series.*, Amsterdam: Elsevier, 2010, pp. 1–144. doi: <https://doi.org/10.1016/B978-0-08-096513-0.00001-7>.
- [6] H. Katagiri, N. Sasaguchi, S. Hando, S. Hoshino, J. Ohashi, and T. Yokota, "Preparation and evaluation of Cu₂ZnSnS₄ thin films by sulfurization of E · B evaporated precursors," *Sol. Energy Mater. Sol. Cells*, vol. 49, no. 1–4, pp. 407–414, Dec. 1997, doi: [10.1016/S0927-0248\(97\)00119-0](https://doi.org/10.1016/S0927-0248(97)00119-0).
- [7] H. Katagiri et al., "Development of CZTS-based thin film solar cells," *Thin Solid Films*, vol. 517, no. 7, pp. 2455–2460, Feb. 2009, doi: [10.1016/j.tsf.2008.11.002](https://doi.org/10.1016/j.tsf.2008.11.002).
- [8] A. Weber et al., "Texture inheritance in thin-film growth of Cu₂ZnSnS₄," *Appl. Phys. Lett.*, vol. 95, no. 4, p. 041904, Jul. 2009, doi: [10.1063/1.3192357](https://doi.org/10.1063/1.3192357).
- [9] X. Song, X. Ji, M. Li, W. Lin, X. Luo, and H. Zhang, "A Review on Development Prospect of CZTS Based Thin Film Solar Cells," *Int. J. Photoenergy*, vol. 2014, p. 613173, May 2014, doi: [10.1155/2014/613173](https://doi.org/10.1155/2014/613173).
- [10] T. Yamaguchi, K. Tsujita, S. Niyama, and T. Imanishi, "Preparation of High Ga Content Cu(In,Ga)Se₂ Thin Films by Sequential Evaporation Process Added In₂S₃," *Adv. Mater. Phys. Chem.*, vol. 02, no. 04, pp. 106–109, 2012, doi: [10.4236/ampc.2012.24B029](https://doi.org/10.4236/ampc.2012.24B029).
- [11] X.-H. Tan, Y. Chen, and Y.-X. Liu, "Silver nanowire composite thin films as transparent electrodes for Cu(In,Ga)Se₂/ZnS thin film solar cells," *Appl Opt*, vol. 53, no. 15, pp. 3273–3277, May 2014, doi: [10.1364/AO.53.003273](https://doi.org/10.1364/AO.53.003273).
- [12] G. Altamura, "Development of CZTSSe thin films based solar cells".
- [13] J.-S. Kim, J.-K. Kang, and D.-K. Hwang, "High efficiency bifacial Cu₂ZnSnSe₄ thin-film solar cells on transparent conducting oxide glass substrates," *APL Mater.*, vol. 4, no. 9, p. 096101, Sep. 2016, doi: [10.1063/1.4962145](https://doi.org/10.1063/1.4962145).
- [14] G. Turgut and E. Sonmez, "A Study of Pb-Doping Effect on Structural, Optical, and Morphological Properties of ZnO Thin Films Deposited by Sol-Gel Spin Coating," *Metall. Mater. Trans. A*, vol. 45, Jul. 2014, doi: [10.1007/s11661-014-2281-6](https://doi.org/10.1007/s11661-014-2281-6).

How to cite this article:

Liaqat Khan, Adnan Duad "Analyzing the Efficiency of CZTSSe Solar Cell With Three Different ETMs" *International Journal of Engineering Works*, Vol. 11, Issue 09, PP. 153-159, September 2024. <https://doi.org/10.34259/ijew.24.1109153159>.

